Calorimetric Measurement of the Heat of Adsorption of Benzene on Pt(111)[†]

Hyeran Ihm, Henry M. Ajo, J. M. Gottfried, P. Bera, and Charles T. Campbell*

Department of Chemistry, Box 351700, University of Washington, Seattle, Washington 98195-1700

Received: February 21, 2004; In Final Form: May 25, 2004

The heat of adsorption of benzene on clean Pt(111) at 300 K is measured calorimetrically and found to decrease with coverage (θ) as $(197 - 48\theta - 83\theta^2)$ kJ/mol. Saturation coverage ($\theta = 1.0$) is 2.3×10^{14} molecules/cm^2. Sticking probabilities of benzene on Pt(111) were measured by mass spectrometry, giving an initial value of 0.97 and showing Kisliuk-type behavior with increasing coverage that implies there is a precursor to sticking with a ratio of its hopping rate to its desorption rate of ~28. Benzene adsorbs transiently on the benzene-saturated surface at 300 K with a trapping probability of 0.90 and a heat of adsorption of 63−73 kJ/mol.

1. Introduction

King's group first reported a calorimeter capable of precise measurements of heats of adsorption on single crystal surfaces, which they called single crystal adsorption calorimetry (SCAC).[1,2] Since then, SCAC has provided adsorption energies for high-vapor-pressure substances (e.g., O_2, CO, NO, and ethylene)[3−10] and metal atoms[11−25] on clean single crystal surfaces. Adsorption energies for low vapor pressure compounds (compounds which are liquids at room temperature and atmospheric pressure) have not previously been measured by SCAC because these require a completely different type of molecular beam than those available on the two single crystal adsorption calorimeters present in the world. These include many molecules of interest in surface chemistry related to catalysis, chemical vapor deposition (CVD) processes, and biochemistry. Here we report for the first time calorimetric measurements of a low vapor pressure compound on a single crystal surface, benzene on Pt(111).

Benzene adsorption has been studied extensively on Pt(111),[26−50] because it is the simplest aromatic hydrocarbon and Pt(111) is the most thermodynamically stable and most widely studied Pt surface, and because of the importance to fossil fuel utilization efficiency of hydrocarbon aromatization reactions performed over Pt catalysts. Thus, its adsorption energy is of substantial fundamental importance. At 300 K, benzene adsorbs molecularly on Pt(111)[30,33,36,43] with its molecular plane parallel to the surface, interacting with the Pt through its aromatic π electron system.[28,29,33,37,51] Thus, its heat of adsorption is 6 times the C−Pt(111) bond energy for a carbon atom in an aromatic ring parallel to the surface. This energy is a number of general interest concerning the thermochemistry of surfaces. This value could be compared, for example, to the C−Pt(111) σ bond energy determined by King's group using the adsorption heat of ethylene on Pt(111).[52]

Benzene adsorbs molecularly on Pt(111) at 300 K, but upon heating coverages below ~0.6 ML (ML = monolayer = saturation coverage at 300 K), it dissociates completely into H_2 gas and adsorbed graphitic carbon before desorbing.[36] Therefore, its adsorption energy cannot be measured with desorption-based methods such as temperature programmed

desorption (TPD), molecular beam relaxation spectroscopy (MBRS), and equilibrium adsorption isotherms, at least below 0.6 ML. Even at higher coverages where a fraction desorbs intact, the TPD and MBRS line shapes are complicated by the competition from dissociation, rendering rigorous data analysis of desorption rates to extract the desorption energy impossible. Even at saturation coverages, only ~45% of the adsorbed benzene desorbs intact, whereas the remainder dehydrogenates,[36] so that the use of equilibrium adsorption isotherms is also impossible. Thus, a direct method like SCAC is required for the measurement of benzene adsorption energies, and that is what we report here.

Despite the problems with analysis of TPD data mentioned above, several reasonable attempts have been made to extract an activation energy for desorption from TPD data for high-coverage benzene on Pt(111) using Redhead analysis and assuming a prefactor for desorption of 10^{13} s^{-1}.[31,33,36,43] This gave values ranging from 133 kJ/mol[36] to 121 kJ/mol.[43] It was assumed that the adsorption energy approximately equals this activation energy, giving

$$\Delta H_{ads} = 133\text{-}121 \text{ kJ/mol} \qquad (1)$$
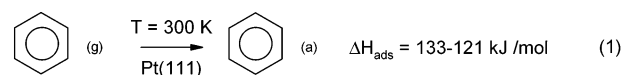
It should be noted that these values are for ~0.8 ML initial coverage. Our calorimetric measurements reported here are consistent with these approximate values, but extend them by showing that the adsorption energy is much higher (up to 197 kJ/mol) at low coverage.

The results also allow us to test an assumption made in our earlier measurements of the ensemble (site size) requirements for the dehydrogenation of a series of cyclic hydrocarbons on Pt(111).[53−56] There, we used low coverages of coadsorbed bismuth atoms to block Pt sites, and quantified the resulting decrease in dehydrogenation rate as a function of Bi coverage. By fitting the data to a kinetic model, we were able to determine the number of unoccupied Pt surface atoms needed for dehydrogenation. That kinetic model relied on an assumption that the low coverages of Bi used had a negligible effect on the desorption rate constant for the adsorbed hydrocarbon. Because the experiments were done at lower coverage where much of the hydrocarbon (all of it in the case of benzene) dehydrogenated

---

instead of desorbing during TPD in the absence of bismuth, it was hard to be sure this was true. It relied on extrapolating high coverage TPD results to low coverage, which is questionable because one could not be sure that the molecules that dehydrogenated did not have a substantially higher adsorption energy than those that desorb at high coverage. The direct measurement here of the heat of adsorption of the adsorbed benzene at low coverage, which dehydrogenates later in TPD allows us to assess the effect of Bi on the adsorption energy (desorption rate) of these species.

2. Experimental Section

The SCAC apparatus will be described elsewhere[57] but is briefly described here. It is the third SCAC in the world. It is unique among these in that it is designed specifically to measure the heats of adsorption of low vapor pressure molecules, such as benzene. Its ultrahigh vacuum (UHV) chamber has capabilities for Auger electron spectroscopy (AES), X-ray photoelectron spectroscopy (XPS), low energy electron diffraction (LEED), and low energy ion scattering spectroscopy (LEIS). The calorimeter design follows that of Dr. D. A. King's group[3−6] but uses a different method of heat detection that we developed and reported earlier.[12−14,17] A 9 μm thick, 4 mm wide pyroelectric polymer ribbon (β-polyvinylidene fluoride, PVDF), with a 50 nm NiAl coating on both sides, is pressed against the back of the single crystal to make good thermal contact. For our calorimetry experiments, we use a chopped, effusive molecular beam running at 0.5 Hz with a pulse width of 100 ms to impinge benzene molecules on the 1 μm thick Pt(111) sample. The heat of adsorption of the benzene molecules causes the temperature of the single crystal to rise. The pyroelectric ribbon's temperature also rises, resulting in a peak in its face-to-face voltage signal. We calibrate this peak size using pulses of a HeNe laser of known energy. We impinge pulses of this laser on the Pt(111) crystal. The ratio of the voltage rise to the amount of laser energy, in joules, deposited in the crystal by the light pulse gives a value in V/J for the sensitivity of this heat detection system. For this calibration, we used the optical reflectivity of 76% for this Pt(111) crystal at the wavelength of the HeNe laser and normal incidence, which we measured using an integrating sphere. The value is slightly larger than previously reported values.[58−60] We divide the calorimetry signal caused by adsorbing each pulse of the benzene molecular beam by this sensitivity factor to convert its voltage to the energy absorbed by the sample, in joules.

The molecular beam is a new design and will be described in detail elsewhere.[57] Briefly, benzene is passed through a room-temperature multichannel array to form a peaked angular distribution, then collimated with several orifices, and chopped into 100 ms pulses with a 2.000 s repeat rate with a mechanical chopper before impinging on the Pt. The differential pumping of this beam system is supplied by its liquid nitrogen cooled orifices and walls, and turbomolecular pumps. The benzene flux within its ~4 mm diameter at the sample was measured as described in ref 57 using a liquid nitrogen cooled, calibrated quartz crystal microbalance (QCM) and also using the sticking probability versus coverage measured with a quadrupole mass spectrometer (QMS) as outlined below. This second method requires knowing the saturation coverage at the sample temperature of 300 K (one monolayer = 1.00 ML), which was reported previously to be 2.3×10^{14} benzenes/cm^2 [31] and 2.4 $\times 10^{14}$ benzenes/cm^2.[36] The correlation between these QCM and QMS methods allowed us to measure the flux after calorimetry runs with the QCM, which did not disturb the very sensitive PVDF ribbon as much as does turning on the QMS.
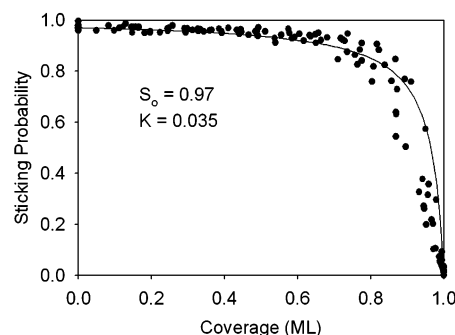

Figure 1. Sticking probability measured for benzene on clean Pt(111) at $T = 300$ K (dots), as well as the best fit to the data using the Kisliuk equation (eq 1), which is a model for precursor-mediated adsorption (solid curve). The parameters in the fit are noted. One ML corresponds to 2.3×10^{14} benzene molecules/cm^2.

The flux was typically 0.07 ML of benzene per pulse here, resulting in the sample being saturated in ~15 pulses.

The sticking probability of the benzene molecules on the Pt(111) surface with each pulse of the molecular beam must be known to determine the fraction of benzene molecules that contribute to the calorimetry signal, necessary for reporting the heats per mole of adsorbing benzene. This was determined by measuring the nonsticking fraction of benzene molecules with a QMS in a line-of-sight modification of the King and Wells method described elsewhere.[14] We found that the sticking probability depends slightly on the flux at high coverages, so we were careful to use a flux similar to that for the calorimetry measurements.

3. Results

3.1. Sticking Probability Measurements of Benzene on Pt(111) at 300 K. The sticking probability measured for benzene on Pt(111) at 300 K as a function of coverage is shown in Figure 1. Included here are data points from many runs, each starting with a clean surface. The initial sticking probability starts out at about ~0.97 and slowly drops, until at a coverage of about 0.9 ML, it drops sharply toward zero. Here, 1.00 ML is defined as the coverage at which the sticking probability drops to zero at 300 K (2.3×10^{14} benzenes/cm^2 as determined in ref 31). The initial sticking probability, S_o, of benzene on Pt(111) has been measured previously to be 1.0 at 100 K[40] and 0.95 at 200 K,[43] but to our knowledge, has not been measured at room temperature. These values are consistent with the present result (0.97 at 300 K), suggesting a nearly temperature-independent sticking probability below 300 K. We have fitted the coverage dependence of the sticking probability with the Kisliuk[61] model, which is a model for precursor-mediated sticking. We assumed that a gas molecule that strikes a previously filled site on the surface is transiently trapped in a weakly adsorbed precursor state with unit probability, from which it can either desorb or diffuse to a neighboring site and chemisorb there, if that new site is empty. According to this model, the sticking probability (S) varies with the fractional coverage of the surface by the adsorbate (θ) as

$$S = \frac{S_o}{1 + K\left(\dfrac{\theta}{1 - \theta}\right)} \quad \text{where} \quad K \approx \frac{k_{\text{desorption}}}{k_{\text{hopping}}}$$

$$\text{when} \quad k_{\text{hopping}} >>>> k_{\text{desorption}}$$

where S_o is the initial sticking probability and K is approximately equal to the kinetic rate constant for desorption, $k_{\text{desorption}}$, divided
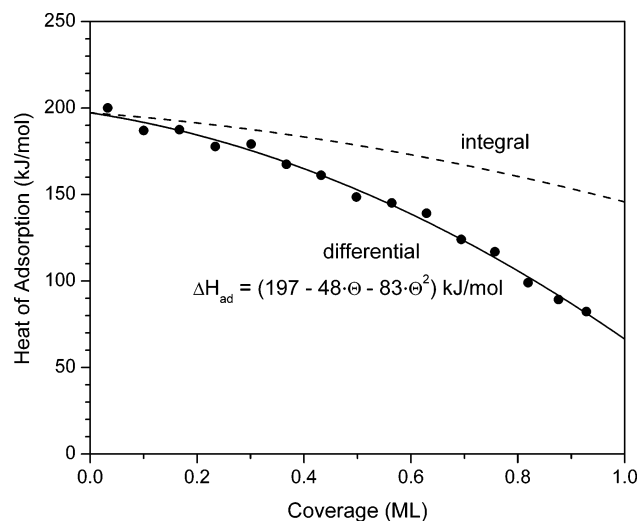
Figure 2. Measured differential heat of adsorption of benzene as a function of coverage on Pt(111) at 300 K (dots). Also shown is the best fit to the data using a second-order polynomial dependence on coverage (solid line). The integral heat of adsorption computed using this polynomial is shown as the dashed curve.

by the kinetic rate constant for hopping, $k_{hopping}$, in both cases for a precursor adsorbed on a filled site. From the best-fit value of K (0.035), we derive that $k_{desorption}/k_{hopping} = 0.035$, meaning that it is ~28 times more likely that such a precursor will hop to another site than desorb.

3.2. Heat of Adsorption Measurements of Benzene/Pt(111) at 300 K. The measured molar heats of adsorption for benzene on clean Pt(111) at $T = 300$ K are presented in Figure 2 as a function of coverage. Each point corresponds to one gas pulse. The data here are the average of two runs, each starting from clean Pt(111). These heats were calculated from our measured calorimetric heats by dividing by the number of moles which stuck in each pulse (i.e., flux times pulse duration times sticking probability) and adding $^1/_2RT$.[2] The resulting heats of adsorption reported here are thus equal to the standard molar enthalpy of adsorption and identical to the isosteric differential heat of adsorption.[2,62]

Figure 2 shows that the differential heat of adsorption decreases smoothly with increasing coverage. The data were well fitted by the second-order polynomial:

$$(197 - 48\theta - 83\theta^2) \text{ kJ/mol}$$

where the coverage (θ) is in units of ML. The standard deviation of the data points about this curve is 1.4%, which gives a measure of the precision of the measurement. We estimate the maximum error in the absolute values of these heats as ~10%, based on our uncertainties in our estimates of the beam flux and the optical reflectivity of our Pt(111) sample, both of which scale the data.

Extrapolating this polynomial fit to zero coverage gives an initial heat of adsorption of 197 kJ/mol, but extrapolating it to 1.0 ML gives only 66 kJ/mol. We attribute this large decrease to repulsive lateral interactions between the benzene molecules and a change of adsorption site as the coverage increases (see below).

Also shown in Figure 2 is the integral heat of adsorption versus coverage, obtained by integrating this polynomial fit from zero coverage.

Table 1 compares the results of Figure 2 with several prior estimates of the enthalpy of benzene adsorption based on TPD or quantum computation. To compare our heats of adsorption

TABLE 1: Isosteric Heats of Adsorption of Benzene on Pt(111)[a]

ΔH_{ad} (kJ/mol)	method of determination	q (ML)	ref
$(197 - 48\theta - 83\theta^2)$	SCAC	0 to 1.0	this paper
123		0.7	
123*		0.6 → 0.8*	
160*		0 → 0.8*	
167*		0 → 0.7*	
133	TPD: Redhead analysis	0.8	36
121	TPD: Redhead analysis	0.8	43
126	TPD: Redhead analysis	0.8**	33
124	TPD: Redhead analysis	0.8**	31
119*	DFT slab calculation	0.7*	50

[a] All values are differential heats of adsorption unless noted with *. Key: *, integral heat of adsorption; **, coverage estimated by comparing TPD spectra to those in ref 36.

to activation barriers for desorption (E_a^{desorb}) from TPD results, one must assume that adsorption is nonactivated (which is a good approximation, because the sticking probability is near unity between 100 and 300 K, see above) and add $^1/_2RT_{desorb}$ to the activation barrier.[7,62] The TPD values are reported at their initial coverages. Desorption energies found in the citation were used when given,[36,43] otherwise peak desorption temperatures[31,33] were converted to desorption energies using first-order Redhead analysis[63] assuming a prefactor of 10^{13} s^{-1}. In those two cases,[31,33] the initial coverages were not given and so they were estimated by comparison of TPD spectra to those in other studies where coverages were reported.[36,43] The average value from TPD results is 126 kJ/mol for 0.8 ML initial coverage.

It is difficult to know the coverage in our measurements to which these TPD values should be compared, because most of the benzene dissociates during TPD for this initial coverage. Assuming that the desorbing fraction is representative of the entire population of benzene on the surface, it would be appropriate to compare the TPD values to our integral (average) heat of adsorption, 160 kJ/mol at 0.8 ML. However, desorption does not begin until the initial coverage exceeds ~0.6 ML, below which all the adsorbed benzene dissociates.[36] Assuming that benzene adsorbed with local coverages below 0.6 ML dissociates completely and that benzene with local coverage above 0.6 ML desorbs completely until the coverage drops to 0.6 ML but dissociates completely thereafter, then one should compare the TPD values to our heat of adsorption integrated (averaged) from 0.6 to 0.8 ML, 123 kJ/mol. In reality, the situation is somewhere between these two limiting cases (but closer to the latter) because desorption and dissociation occur to some extent simultaneously rather than perfectly sequentially. It is further complicated by the fact that the dissociation product remaining on the surface (C_2H^{36}) may have a different energy of interaction with coadsorbed benzene. These problems highlight the difficulties encountered in trying to analyze TPD data whenever dissociation competes significantly with molecular desorption, and the advantage of direct calorimetric measurement. Furthermore, the TPD values may be biased toward lower values by use of an incorrect prefactor, which could easily be several orders of magnitude larger than assumed.[64]

Prior TPD data showed a poorly resolved shoulder for molecular benzene desorption (the β peak at ~350 K) that populates just before 1 ML coverage, with a desorption activation energy of ~88 kJ/mol (estimated assuming prefactor of 10^{13} s^{-1}), 30% lower than the dominant TPD peak (α, at 505 K).[54] After adding $^1/_2RT_{desorb}$, this gives a heat of adsorption of 87 kJ/mol. This equals the differential heat measured calorimetrically here at 0.9 ML, consistent with the coverage range over which this shoulder is seen in TPD.
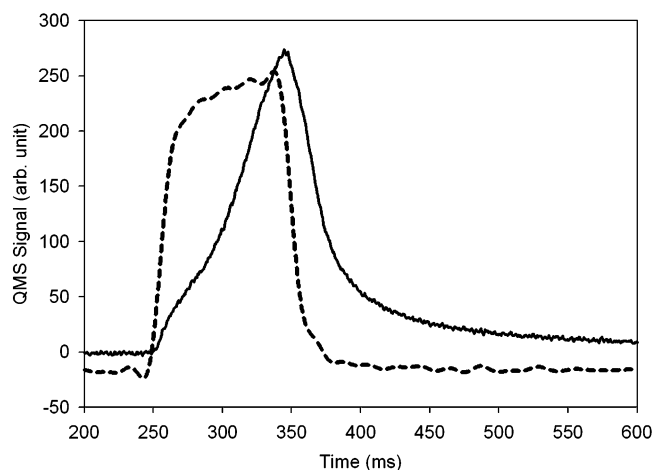
Figure 3. Comparison of measured QMS signal for benzene molecular beam pulses scattered from the Pt surface, averaged for all the pulses below 0.9 ML (dashed line, smoothed by Fourier-filtering out noise above 50 Hz, and magnified 6 times) and for 30 pulses after saturation (solid line, without smoothing).

To compare Figure 2 to theoretical results, one must integrate these differential heats of adsorption from zero up to the coverage of the structure used for the theoretical calculation. Density functional calculations at 0.7 ML gave a value of 119 kJ/mol,[50] 30% lower than our *integral* heat of adsorption of 167 kJ/mol at this coverage.

3.3. Dynamics of Benzene Adsorption. Figure 3 shows the line shapes of the QMS signal for the molecules that did not stick on the surface, as measured to obtain the sticking probability in Section 3.1. The dashed curve is the average line shape for coverages below 0.9 ML. This is very similar to the line shape measured for the direct molecular beam before scattering off the Pt, which is, however, flatter on the top. This shows that most molecules that do not stick on the surface below 0.9 ML either scatter quasi-elastically from the surface (possibly at impurities) or have a smaller residence time when transiently adsorbed than the time resolution of our chopper blade's cutoff (~10 ms). The solid curve is the line shape after saturation. It shows that the molecules that do not stick for the whole 2.00 s period of a pulse actually do stick transiently on the surface, as evidenced by both the missing intensity during the first 150 ms of the beam "on" time, and the extended tail due to desorption after the beam is completely "off". This line shape can be decomposed into a portion that has zero residence (i.e., follows the incoming beam's line shape, as measured by reflecting the beam off a hot gold surface) and a portion that sticks to the Pt and has long residence time, as shown in Figure 4.

Let us define the condensation coefficient as the entire portion of benzene molecules sticking to the Pt surface both permanently and transiently (equal to 1.00 minus the fraction that has zero residence time). This condensation coefficient for each pulse was calculated from line shape decompositions such as shown in Figure 4 and is presented versus coverage in Figure 5. Even when the sticking probability drops to zero after saturation, the condensation coefficient (transient trapping probability) stays at ~0.90.

The average residence time of the benzene molecules that get transiently adsorbed on the Pt surface after saturation was determined by fitting the decreasing tail portions of the QMS signal in Figure 4 to an exponential decay function. The fit was poor, but a double exponential decay fit this tail very well: r_1 $\exp(-t/\tau_1) + r_2 \exp(-t/\tau_2)$. The best fit gave $r_1 = 244$ and $r_2 = 535$ (in the same units as the QMS signal), and residence
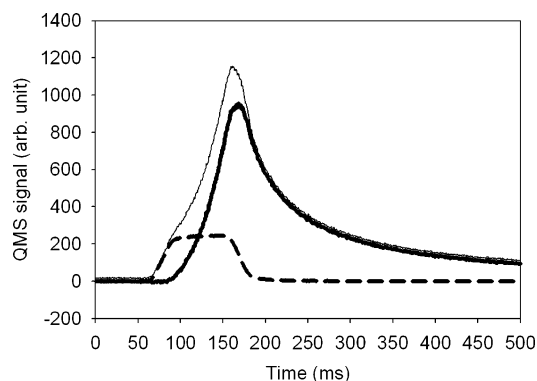

Figure 4. Decomposition of the measured QMS signal for benzene molecular beam pulses scattered from the Pt surface, averaged for 40 benzene pulses after saturation (thin solid curve) into (a) the benzene molecules that never stuck to the surface (dashed curve) and (b) the benzene molecules that initially adsorbed but desorbed from the surface within the 2.0 s period of the pulse (wide solid curve).
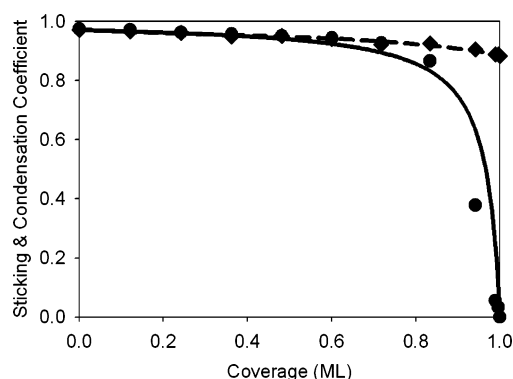

Figure 5. Comparison of sticking probability (filled circle) and condensation coefficient (filled diamond) of benzene on the Pt surface at 300 K. The solid line is the fit to a Kisliuk model and the dashed line is a guide to the eye for the condensation coefficient.

times $\tau_1 = 703$ ms and $\tau_2 = 101$ ms. These values imply that ~75% and 25% of the transiently adsorbed molecules at saturation have characteristic residence times of 703 ms and 101 ms, respectively. Because $1/\tau_i = k_{d,i} = \nu_{d,i} \exp(-E_{d,i}/RT)$, we can extract from these values a value for the activation energy for desorption, $E_{d,i}$, if we assume a value for $\nu_{d,i}$ of 10^{13} s^{-1}. The desorption energies at saturation thus were determined to be as 74 and 69 kJ/mol, respectively. The reason that two residence times are observed may be associated with surface heterogeneity, with the longer time perhaps, for example, corresponding to molecules which visit, during their residence time on the surface, a local environment where the local benzene coverage is lower, or a saturated step edge (which may bind this high-coverage benzene state more strongly). The approach of these residence times and desorption energies (for the nonsticking fraction) to their saturation values with coverage, for coverages just below saturation, are shown in Figure 6.

Figure 7 compares the line shapes of the raw calorimetry voltage peaks before saturation and after saturation of the Pt surface by benzene, for the peaks used to get the heats reported in Figure 2. The line shape before saturation is the same as for those obtained due to light pulses during calibration of the calorimeter, and thus these peak heights can be converted to a heat of adsorption based on that calibration (see above). However, the line shape is markedly different after saturation, so such a simple analysis is not valid. The (unscaled) signal after saturation decreases more rapidly than before saturation, due to a negative heat contribution due to the transiently
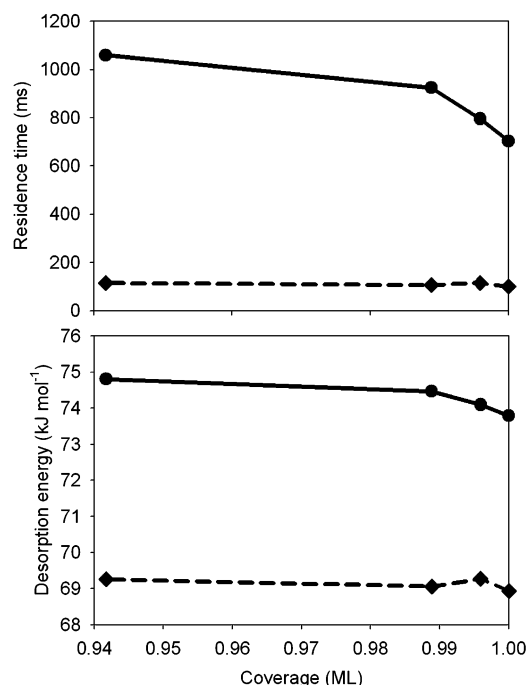
Figure 6. Residence times (top) and desorption energies (bottom) versus coverage near saturation estimated from a double-exponential fit to the QMS signal for the transiently adsorbed molecules which do not permanently stick on the surface (as in Figures 4 and 5).
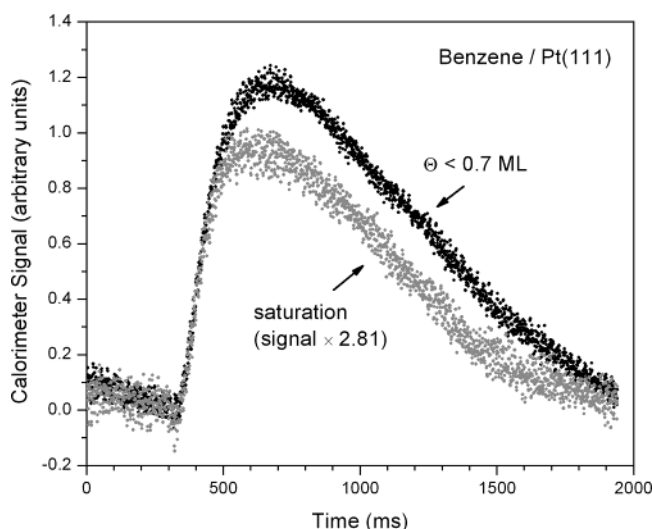

Figure 7. Peak shapes for calorimetry signal from benzene on Pt(111), averaged for all pulses up to 0.7 ML and for ~20 pulses after saturation, scaled so that the initial slopes of the heat response are equal.

adsorbed molecules desorbing from the surface at these times during the pulse (see QMS pulse shapes in Figures 3−4). However, there is no contribution from this effect during the initial rise of the heat signal, so the slopes of these leading edges should be proportional to the heat deposited into the sample per unit time. The slope of the leading edge of the average calorimetry signal before saturation is 2.81 times that of the signal after the saturation. (Note the scaling factor of 2.81× on the latter curve in Figure 7.) By assuming that these slopes are proportional to the heats of adsorption times the condensation coefficient (from Figure 5), we can estimate the heat of adsorption of benzene after saturation to be 63 kJ/mol. The calorimetry signal line shape before saturation is an average of all pulses up to 0.7 ML, where the average (integral) adsorption energy is 167 kJ/mol and the average sticking probability is 0.95. The accommodation coefficient after saturation is 0.90.

Interestingly, this value of 63 kJ/mol agrees almost perfectly with the differential heat of adsorption obtained by extrapolating the polynomial fit of the heat data in Figure 2, which gives 66 kJ/mol at 1.0 ML. These values are also close to the population-weighted average value of ~73 kJ/mol estimated above from surface residence times at saturation. For comparison, the heat of sublimation of benzene (~44 kJ/mol[65]) is considerably smaller.

4. Discussion

The initial heat of adsorption for benzene on Pt(111) of 197 kJ/mol allows us to estimate an average C−Pt bond energy. It is known that benzene adsorbs molecularly on Pt(111) at this temperature and coverage in a structure parallel to the surface.[28,29,33,37,51] Thus, dividing this adsorption energy by six provides the average energy of the C−Pt(111) bonds that hold this aromatic ring to the surface. This bonding is associated with the σ donation of electrons from the carbon atoms' sp^2 orbitals into antibonding Pt orbitals (with some π-back-bonding as well), where these sp^2 orbitals are still dominated by their intramolecular C−C π bonding in benzene's aromatic ring. These C−Pt(111) bonds thus have an average energy of 197/6 = ~33 kJ/mol. In principle, this value could be used to estimate the adsorption energy of other species on Pt(111) wherein the mechanism of bonding of C atoms is similar. This bond energy is 7-fold weaker than the Pt−C σ bond strength of about 230−250 kJ/mol determined for species such as di-σ-bonded ethylene and tri-σ-bonded ethylidyne on Pt surfaces.[66]

The highest possible coverage at which benzene molecules can be packed onto the surface in identical adsorption sites parallel to the surface without overlapping their van der Waals radii is one benzene for every seven Pt(111) surface atoms, corresponding to a ($\sqrt{7} \times \sqrt{7}$)R19° surface lattice. This coverage equals 0.94 ML for our definition of 1.0 ML.

The adsorption heat in Figure 2 was found to decrease with coverage as $(197 - 48\theta - 83\theta^2)$ kJ/mol. Perrson[67] has shown how this functional dependence can arise within a simple lattice site model from pairwise interaction energies, assuming immobile adsorbates but allowing the adsorbates to move slightly out of the site centers to relax nearest-neighbor repulsions. However, at high coverage, they are constrained from doing so by other surrounding (third-body) benzenes. For a hexagonal lattice with only nearest neighbor interactions, our *initial* heat (197 kJ/mol) would equal Perrson's parameter, μ, the adsorption energy of an isolated benzene. The first-order coefficient (48 kJ/mol) would equal Perrson's $6(V_0 - 2\epsilon)$ and the second-order coefficient (83 kJ/mol) would equal 12ϵ, where V_0 is the pairwise repulsion when neighboring benzenes are centered on nearest-neighbor sites, and 2ϵ is the relaxation of repulsion that occurs when both benzenes in an isolated, nearest-neighbor benzene pair move slightly off of their site centers, to reduce their pairwise repulsion and minimize their total energy. When analyzed within this model, the calorimetric data give $V_0 = 21.8$ kJ/mol for the nearest-neighbor repulsion and $2\epsilon = 13.8$ kJ/mol for the extent to which this repulsion is relaxed in an isolated pair. The pairwise repulsion may arise from direct steric interactions, dipole−dipole interactions, and/or strain in the Pt(111) surface induced by adsorbed benzene, which acts in the direction opposite to that of its nearest-neighbor benzene. Of course, the presence of any defect sites such as step edges that bind benzene more strongly would complicate this interpretation.

It is reasonable to assume that this transiently adsorbed state probed in Figure 6 is the transient precursor that is involved in

populating the α state of benzene at lower coverages, made obvious by the sticking probability measurements of Figure 1. Its population-averaged residence time at the lowest coverage measured (Figure 6) is ~820 ms, corresponding to a desorption rate constant of 1.2 s^{-1} for this precursor at 300 K. The best-fit value of K (0.035) to Figure 1 showed that it is ~28 times more likely that this precursor will hop to another site than desorb at 300 K. Multiplying this by its desorption rate constant provides an estimate of its hopping rate constant, giving ~34 s^{-1} at 300 K. Assuming a prefactor of 10^{13} s^{-1}, this corresponds to an activation energy for precursor hopping of 66 kJ/mol. Surprisingly, this is 90% of its adsorption energy. This large activation energy for hopping may be associated with the geometry of this precursor (at least in the structure which dominates its residence time on the surface), which is probably benzene squeezed between other benzene molecules so that it too can bind to the underlying Pt.

The strong decrease in adsorption energy with coverage at high coverages (Figure 2) may explain the need to use a double exponential (two desorption energies) to fit the data of Figures 4 and 6. Note that the coverage decreases by ~5−10% of a ML during the fitted transient in Figure 4.

Our group has previously estimated the number of unoccupied Pt surface atoms needed (i.e., the Pt ensemble requirement) for the dehydrogenation of a series of cyclic hydrocarbons on Pt(111).[53−56] By quantifying the decrease in dehydrogenation rate due to the coadsorbed bismuth atoms as a function of Bi coverage, we estimated the number of unoccupied Pt surface atoms needed for dehydrogenation. That estimate required a kinetic model that assumed the low Bi coverage had a negligible effect on the desorption rate constant (adsorption energy) for the coadsorbed hydrocarbon.

Because the Bi strongly suppresses dehydrogenation, benzene's adsorption energy in the presence of low Bi coverage can be estimated by Redhead analysis of the benzene TPD peak temperature at that condition (510 K at a benzene coverage of ~0.5 ML[54]) assuming a prefactor of 10^{13} s^{-1}. This gives an activation energy for desorption and heat of adsorption of 130 and 132 kJ/mol, respectively. Because little dissociation occurs in the presence of this added Bi, the TPD peak temperature for benzene at this condition should reflect the integral adsorption energy at 0.5 ML benzene. The direct measurement here of the integral heat of adsorption at 0.5 ML is 180 kJ/mol from Figure 2. This is 36% larger than that estimated from the peak temperature of 510 K. This difference could be entirely attributable to a poor assumption of prefactor: A value of 8 × 10^{17} s^{-1} would give perfect agreement. Nevertheless, the TPD peak temperature at 0.8 ML in the absence of Bi was very similar, 505 K.[54] As noted above, the adsorption energy in this condition should probably be compared to the average adsorption energy between about 0.5 and 0.8 ML. Given the strong dependence of benzene's adsorption heat on coverage in Figure 2, one would expect much more than a 5 K temperature shift in the TPD peak temperatures between these two cases. (That is, the 0.5 ML case with Bi should have had a much higher desorption peak temperature than 510 K, if Bi had had a negligible effect on benzene's desorption energy, unless the prefactor for desorption depends strongly on coverage.) This suggests that low Bi coverage may substantially decrease the adsorption energy (desorption rate) of benzene, thus calling into question the ensemble size requirements reported in.[53−56] Direct measurements of benzene adsorption energies in the presence of Bi would be required to confirm this.

5. Conclusions

The heat of adsorption of benzene on Pt(111) at 300 K is found to be (197 − 48θ − 83θ²) kJ/mol, where θ is the fractional coverage of the surface by benzene. Saturation coverage (θ = 1.0) at 300 K corresponds to 2.3 × 10^{14} molecules/cm².[31] Sticking probability measurements of benzene on Pt(111) give an initial sticking probability of 0.97 and show Kisliuk-type precursor-mediated sticking with a ratio of the hopping rate to the desorption rate of a precursor molecule equal to ~28. After saturation, benzene adsorbs transiently into a weakly held state with an accommodation coefficient of 0.90. The heat of adsorption of this transiently adsorbed state is ~68 ± 5 kJ/mol.

Note Added after ASAP Posting. This article was posted ASAP on 7/27/2004. Three numerical values were changed in the third paragraph of the Discussion Section. The correct version was posted on 7/30/2004.

References and Notes

(1) Borroni-Bird, C. E.; King, D. A. *Rev. Sci. Instrum.* **1991**, *62*, 2177−2185.

(2) Stuckless, J. T.; Frei, N. A.; Campbell, C. T. *Rev. Sci. Instrum.* **1998**, *69*, 2427−2438.

(3) Borroni-Bird, C. E.; Al-Sarraf, N.; Andersson, S.; King, D. A. *Chem. Phys. Lett.* **1991**, *183*, 516.

(4) Borroni-Bird, C. E.; King, D. A. *Rev. Sci. Instrum.* **1991**, *62*, 2177.

(5) Al-Sarraf, N.; Stuckless, J. T.; King, D. A. *Nature* **1992**, *360*, 243.

(6) Al-Sarraf, N.; Stuckless, J. T.; Wartnaby, C. E.; King, D. A. *Surf. Sci.* **1993**, *283*, 427.

(7) Stuckless, J. T.; Al-Sarraf, N.; Cartnaby, C.; King, D. A. *J. Chem. Phys.* **1993**, *99*, 1.

(8) Al-Sarraf, N.; King, D. A. *Surf. Sci.* **1994**, *307−309*, 1−7.

(9) Dixon-Warren, S. J.; Kovar, M.; Wartnaby, C. E.; King, D. A. *Surf. Sci.* **1994**, *307−309*, 16−22.

(10) Stuck, A.; Wartnaby, C. E.; Yeo, Y. Y.; King, D. A. *Phys. Rev. Lett.* **1995**, *74*, 578−581.

(11) Starr, D. E.; Diaz, S. F.; Musgrove, J. E.; Ranney, J. T.; Bald, D. J.; Nelen, L.; Ihm, H.; Campbell, C. T. *Surf. Sci.* **2002**, *515*, 13−20.

(12) Stuckless, J. T.; Starr, D. E.; Bald, D. J.; Campbell, C. T. *J. Chem. Phys.* **1997**, *107*, 5547.

(13) Stuckless, J. T.; Starr, D. E.; Bald, D. J.; Campbell, C. T. *Phys. Rev. B* **1997**, *56*, 13496.

(14) Stuckless, J. T.; Frei, N. A.; Campbell, C. T. *Rev. Sci. Instrum.* **1998**, *69*, 2427−2438.

(15) Ranney, J. T.; Starr, D. E.; Musgrove, J. E.; Bald, D. J.; Campbell, C. T. *Faraday Discuss.* **1999**, *114*, 195−208.

(16) Campbell, C. T.; Grant, A. W.; Starr, D. E.; Parker, S. C.; Bondzie, V. E. *Top. Catal.* **2000**, *14*, 43−51.

(17) Stuckless, J. T.; Frei, N. A.; Campbell, C. T. *Sensors Actuators* **2000**, *B62*, 13−22.

(18) Larsen, J. H.; Ranney, J. T.; Starr, D. E.; Musgrove, J. E.; Campbell, C. T. *Phys. Rev.* **2001**, *B63*, 195410 (8 pp).

(19) Larsen, J. H.; Starr, D. E.; Campbell, C. T. *J. Chem. Thermodyn.* **2001**, *33*, 333−45.

(20) Starr, D. E.; Bald, D. J.; Musgrove, J.; Ranney, J.; Campbell, C. T. *J. Chem. Phys.* **2001**, *114*, 3752−64.

(21) Starr, D. E.; Campbell, C. T. *J. Phys. Chem.* **2001**, *B105*, 3776−82.

(22) Starr, D. E.; Ranney, J. T.; Larsen, J. H.; Musgrove, J. E.; Campbell, C. T. *Phys. Rev. Lett.* **2001**, *87*, art. no.-106102.

(23) Campbell, C. T.; Starr, D. E. *J. Am. Chem. Soc.* **2002**, *124*, 9212−18.

(24) Campbell, C. T.; Parker, S. C.; Starr, D. E. *Science* **2002**, *298*, 811−814.

(25) Campbell, C. T.; Starr, D. E. *J. Am. Chem. Soc.* **2002**, *124*, 9212−9218.

(26) Sautet, P.; Bocquet, M. L. *Surf. Sci.* **1994**, *304*, L445−L450.

(27) Sautet, P.; Bocquet, M. L. *Phys. Rev. B* **1996**, *53*, 4910−4925.

(28) Lehwald, S.; Ibach, H.; Demuth, J. E. *Surf. Sci.* **1978**, *78*, 577−590.

(29) Netzer, F. P.; Matthew, J. A. D. *Solid State Commun.* **1979**, *29*, 209−213.

(30) Tsai, M. C.; Friend, C. M.; Muetterties, E. L. *J. Am. Chem. Soc.* **1982**, *104*, 2539−2543.

(31) Tsai, M. C.; Muetterties, E. L. *J. Am. Chem. Soc.* **1982**, *104*, 2534−2539.

(32) Anderson, A. B.; Mcdevitt, M. R.; Urbach, F. L. *Surf. Sci.* **1984**, *146*, 80−92.

(33) Abon, M.; Bertolini, J. C.; Billy, J.; Massardier, J.; Tardy, B. *Surf. Sci.* **1985**, *162*, 395−401.

(34) Mate, C. M.; Somorjai, G. A. *Surf. Sci.* **1985**, *160*, 542−560.

(35) Ogletree, D. F.; Vanhove, M. A.; Somorjai, G. A. *Surf. Sci.* **1987**, *183*, 1−20.

(36) Campbell, J. M.; Seimanides, S.; Campbell, C. T. *J. Phys. Chem.* **1989**, *93*, 815−826.

(37) Wander, A.; Held, G.; Hwang, R. Q.; Blackman, G. S.; Xu, M. L.; Deandres, P.; Vanhove, M. A.; Somorjai, G. A. *Surf. Sci.* **1991**, *249*, 21−34.

(38) Henn, F. C.; Diaz, A. L.; Bussell, M. E.; Hugenschmidt, M. B.; Domagala, M. E.; Campbell, C. T. *J. Phys. Chem.* **1992**, *96*, 5965−5974.

(39) Hugenschmidt, M. B.; Diaz, A. L.; Campbell, C. T. *J. Phys. Chem.* **1992**, *96*, 5974−5978.

(40) Jiang, L. Q.; Koel, B. E. *J. Phys. Chem.* **1992**, *96*, 8694−8697.

(41) Weiss, P. S.; Eigler, D. M. *Phys. Rev. Lett.* **1993**, *71*, 3139−3142.

(42) Xu, C.; Koel, B. E. *Surf. Sci.* **1994**, *304*, 249−266.

(43) Xu, C.; Tsai, Y. L.; Koel, B. E. *J. Phys. Chem.* **1994**, *98*, 585−593.

(44) Haq, S.; King, D. A. *J. Phys. Chem.* **1996**, *100*, 16957−16965.

(45) Peck, J. W.; Koel, B. E. *J. Am. Chem. Soc.* **1996**, *118*, 2708−2717.

(46) Yimagawa, M.; Fujikawa, T. *Surf. Sci.* **1996**, *358*, 131−134.

(47) Koel, B. E.; Blank, D. A.; Carter, E. A. *J. Mol. Catal. A: Chem.* **1998**, *131*, 39−53.

(48) Manner, W. L.; Girolami, G. S.; Nuzzo, R. G. *J. Phys. Chem. B* **1998**, *102*, 10295−10306.

(49) Weiss, K.; Gebert, S.; Wuhn, M.; Wadepohl, H.; Woll, C. *J. Vac. Sci. Technol. A: Vac. Surf. Films* **1998**, *16*, 1017−1022.

(50) Saeys, M.; Reyniers, M. F.; Marin, G. B.; Neurock, M. *J. Phys. Chem. B* **2002**, *106*, 7489−7498.

(51) Johnson, A. L.; Muetterties, E. L.; Stohr, J. *J. Am. Chem. Soc.* **1983**, *105*, 7183−7185.

(52) Yeo, Y. Y.; Stuck, A.; Wartnaby, C. E.; King, D. A. *Chem. Phys. Lett.* **1996**, *259*, 28−36.

(53) Campbell, C. T.; Campbell, J. M.; Dalton, P. J.; Henn, F. C.; Seimanides, S. G. *J. Phys. Chem.* **1989**, *93*, 806−814.

(54) Campbell, J. M.; Seimanides, S. G.; Campbell, C. T. *J. Phys. Chem.* **1989**, *93*, 815−826.

(55) Rodriguez, J. A.; Campbell, C. T. *J. Phys. Chem.* **1989**, *93*, 826−835.

(56) Henn, F. C.; Dalton, P. J.; Campbell, C. T. *J. Phys. Chem.* **1989**, *93*, 836−846.

(57) Ajo, H. M.; Ihm, H.; Campbell, C. T. *Rev. Sci. Instrum.*, in press.

(58) *Handbook of optical constants of solids, c1998*; Palik, E. D., Ed.; Academic Press: Orlando, FL, 1985; pp 5 v.

(59) Sokolov, A. V. Optical properties of metals. Chomet, S., Translator; In *Optical properties of metals*; Heavens, O. S., Ed.; American Elsevier Publishing Co.: New York, 1967; pp xvii, 472 p.

(60) Weaver, J. H. *Phys. Rev. B* **1975**, *11*, 1416−1425.

(61) Kisliuk, P. *J. Phys. Chem. Solids* **1957**, *3*, 95−101.

(62) Ge, Q. F.; Kose, R.; King, D. A. *Adv. Catal.* **2000**, *45*, 207−259.

(63) Redhead, P. A. *Vacuum* **1962**, *12*, 203-211.

(64) Campbell, C. T.; Sun, Y.-K.; Weinberg, W. H. *Chem. Phys. Lett.* **1991**, *179*, 53−57.

(65) *CRC Handbook of Chemistry and Physics*, 77th ed.; Lide, D. R., Ed.; CRC Press: Boston, 1996.

(66) Brown, W. A.; Kose, R.; King, D. A. *Chem. Rev.* **1998**, *98*, 797−831.

(67) Persson, B. N. J. *Surf. Sci.* **1991**, *258*, 451.